Cascade evolution and radiative recombination of quantum dot multiexcitons studied by time-resolved spectroscopy

E. Dekel, D. V. Regelman, D. Gershoni, and E. Ehrenfreund
Physics Department and Solid State Institute, Technion–Israel Institute of Technology, Haifa 32000, Israel

W. V. Schoenfeld and P. M. Petroff
Materials Department, University of California, Santa Barbara, California 93106
(Received 1 May 2000)

We resolve spatially, spectroscopically, and temporally the photoluminescence emission from single self-assembled InAs/GaAs quantum dots. The rich photoluminescence spectrum and its evolution with time after pulse excitation and with the density of excitation is experimentally measured and analyzed using a theoretical multiexciton model. The model accounts quantitatively for the dynamics of a small number of interacting electrons and holes confined in optically excited semiconductor quantum dots.

I. INTRODUCTION

Optical studies of semiconductor quantum dots in general[1–5] and self-assembled quantum dots in particular[6–11] have been a subject of very intensive investigations for quite some time. These reports brought strong spectral evidence that the presence of few confined carriers in such a small volume gives rise to correlated few-carrier multiplexes, which are unstable otherwise.

In our previous publications we reported on optical investigations of single InAs/$Al_xGa_{1-x}As$ self-assembled strained quantum dots (SAQDs).[10,11] We demonstrated there that the radiative recombination processes in these three dimensionally confined systems are fundamentally different from the recombination processes in systems of higher dimensionality. Specifically, it was established that confined carriers exchange terms are most instrumental for the understanding of the experimental results when more than two carriers of the same type participate in the radiative process.[10–13]

The previously studied, aluminum contained, InAs/$Al_xGa_{1-x}As$ SAQDs (Refs. 10 and 11) have very efficient nonradiative decay channels, which drastically affect the PL efficiency, particularly at low excitation density. These channels, which are due to the presence of Al atoms within the SAQD $Al_xGa_{1-x}As$ hosting layers,[14] are avoided in the present work where In(Ga)As/GaAs SAQD are studied. We present continuous-wave (cw) and time-resolved spectroscopical studies of the dynamics and recombination processes of photogenerated carriers confined in single In(Ga)As/GaAs SAQDs. In these dots, the nonradiative decay rates are greatly reduced. Their significantly enhanced PL emission makes it easier to optically study them and to facilitate time-correlated single photon counting techniques.[1,15–18]

The previously developed theoretical model[11] is extended here to quantitatively analyze our new low light level time-correlated single photon counting of the PL from single SAQDs. Our model systematically explains the measured cw and time-resolved PL spectra and it quantitatively accounts for the dependence of the PL spectra on time and on excitation density. In particular, it accounts for the dynamics of the photoexcited carriers and determines the radiative decay rates of the correlated excitons (''multiexcitons'').

The paper is organized as follows. In Sec. II we briefly discuss the samples and the experimental system. In Sec. III we present our experimental data and in Sec. IV we extend the multiexciton theoretical model. In Sec. V we discuss our measurements and analyze them in terms of the extended multiexciton model. Our conclusions are briefly summarized in Sec. VI.

II. SAMPLES AND EXPERIMENTAL SETUP

A. Samples

The SAQD sample under investigation was fabricated by molecular-beam epitaxy of a strained epitaxial layer of InAs on a (100) oriented GaAs substrate. Small islands connected by a very thin wetting layer are thus formed during the deposition of the strained InAs layer in the Stranski-Krastanov[19] growth mode. These islands form high-quality QDs with diameters of less than 50 nm when they are capped by an epitaxial layer of GaAs. The vertical and lateral dimensions of the InAs SAQDs were adjusted during growth by the partially covered island growth technique.[20] This technique was applied for the deposition of a 3-nm-thick GaAs cap layer at 530 °C on the InAs SAQDs, thus fixing their height. The growth sequence was then terminated with the deposition of a GaAs cap layer at an elevated growth temperature of 560 °C. Atomic force microscopy was used to determine the dimensions of the uncapped reference sample. The dots were found to have base dimensions of 45 nm by 40 nm and height of 4.5 nm. During the growth of the SAQD layer, the sample was not rotated, forming thus a gradient in the QDs density. In particular, low density areas, in which the average distance between neighboring QDs is larger than our optical spatial resolution, could easily be found on the sample surface.

B. Experimental setup

We use a diffraction-limited low-temperature confocal optical microscope for the photoluminescence (PL) studies

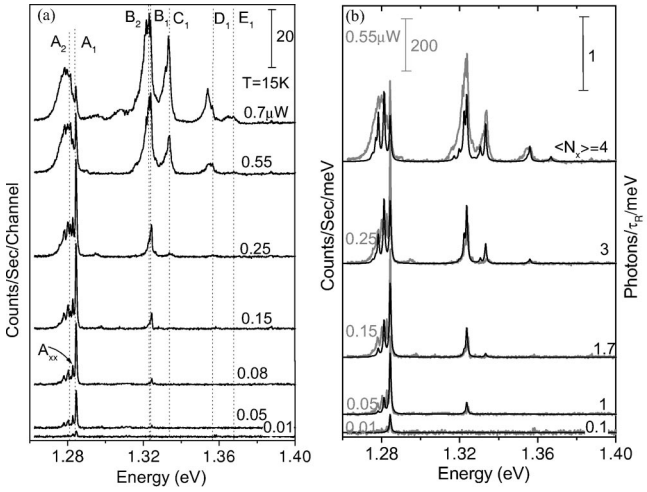

FIG. 1. Measured (a, and gray solid lines in b) and calculated (b, black solid lines, right axis) single SAQD PL spectra at various cw excitation powers. The spectra are vertically shifted for clarity.

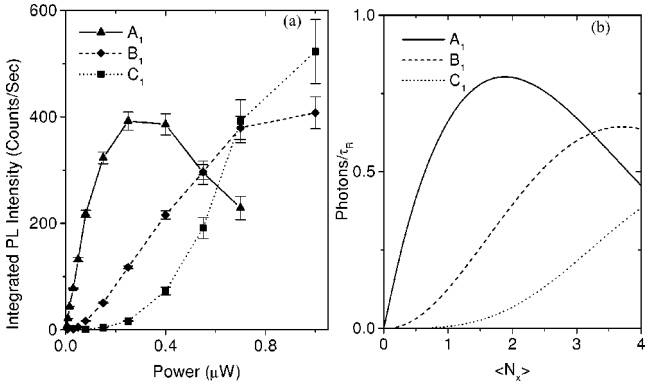

FIG. 2. Measured (a) and calculated (b) spectrally integrated PL emission intensity as a function of cw excitation power (a) and steady-state number of photogenerated QD excitons (b) for various spectral lines from Fig. 1.

of the single SAQDs. The setup is described in detail elsewhere.[11] We used an X60 *in situ* microscope objective in order to focus Ar-ion, tunable Ti:sapphire, or dye laser light at normal incidence on the sample. Both cw and picosecond pulsed excitations were used. The emitted light was collected by the same microscope objective which was accurately manipulated in three directions using computer-controlled motors. A CCD camera based active feedback loop was used for stabilizing the objective-sample working distance. The collected light was spatially filtered, dispersed by a 0.22 m monochromator, and detected by a nitrogen-cooled CCD array detector. The system provides diffraction-limited spatial resolution, both in the excitation and the detection channels. The spatial full width at half maximum of a single QW PL emission intensity was found to be 0.5–0.6 μm, in agreement with the expected diffraction-limited optical resolution at this wavelength ($\simeq$750 nm). The collection efficiency of our system was carefully determined from the measured spectrum of the reflected laser beam. For the time-resolved spectroscopy, the dispersed light from the monochromator was focused onto a small, thermoelectrically cooled, single channel avalanche silicon photodiode. The signal from the photodiode was analyzed using conventional photon counting electronics. The photodiode dark count rate is 100 $\sec^{-1}$ and the system temporal resolution is 200 ps.

III. EXPERIMENTAL RESULTS

We locate an optically excited SAQD by scanning the sample surface while monitoring the resulting PL spectra. Once a typical emission spectrum from an SAQD is observed, the scan is terminated and the objective position is optimized above the dot while verifying that the emitting area is indeed limited by our system's spatial resolution.

In Fig. 1(a) we display typical PL spectra from a single SAQD for various cw excitation powers at photon energy of 2.25 eV. At the lowest excitation density (0.01 μW), a single narrow spectral line is observed at an energy of 1.284 eV. We denote this line by A_1. Its linewidth at this excitation density is limited by the spectral resolution of our system (0.2 meV). As the excitation density increases, two notable changes in the PL spectrum occur. First, a satellite spectral line, A_2, appears 3.5 meV below A_1. In some cases, an additional spectral line, which we denote by A_{xx}, accompanies the appearance of A_2. This line, which is about 1 meV below A_1, is not always spectrally resolved. Second, a higher-energy spectral line, B_1, emerges at 1.324 eV, 40 meV above the first line to be observed, A_1. At yet higher excitation powers, an additional spectral line, B_2, develops 1.5 meV lower in energy than B_1. Further increase in the excitation power results in an increase in the number of satellites, gradually forming spectral emission bands to the lower-energy side of the lines A_1 and B_1, respectively. In addition, new higher-energy groups of spectral lines, *C*, *D*, and *E*, respectively, gradually emerge and similarly develop their own satellites and lower-energy spectral bands. For clarity, we mark the various spectral lines by letters and numerical subscripts, representing, respectively, the energy group to which the spectral lines belong and their appearance order with increasing excitation density. For instance, A_1 denotes the bluest line in group *A*, and B_2 is the first satellite line in group *B*.[21]

With the increase in power, all the observed lines at their appearance order undergo a cycle in which their emission intensity first increases, then reaches maximum and saturates, and eventually, at yet higher excitation powers, the emission intensity significantly weakens. As a result, since the higher-energy lines in each spectral group are the first to appear, they are also the first to lose strength. Consequently, the various groups seem to be ''redshifted'' with the increase in excitation power. Our model simulations (see below), which are presented for comparison in Fig. 1(b), (solid black lines, right axis) overlaid on the experimental measurements (solid gray lines, left axis), duplicate this behavior.

The evolution of the PL spectrum with increasing excitation power is shown in Fig. 2(a), where the measured integrated emission intensity of three of the spectral lines is plotted as a function of the excitation power on the QD. The calculated (see below) integrated PL as a function of the average number of steady-state excitons, $\langle N_x \rangle$, in the QD, presented for comparison in Fig. 2(b), accurately describes this evolution. We note also that, with the knowledge of our experimental setup efficiency, Fig. 2 can be used in order to

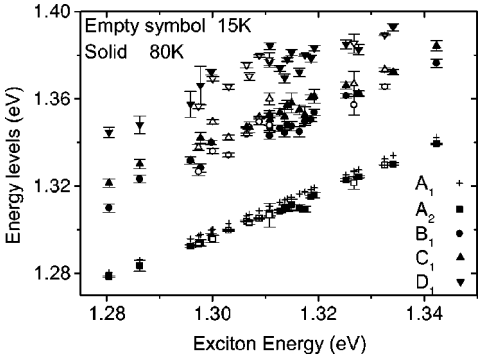

FIG. 3. PL emission energy of various spectral lines vs the energy of the A_1 line for various SAQDs.

accurately determine the radiative rate of a single QD exciton τ_R^{-1} (see below).

Figure 3 presents a compilation of the energies of all the observed spectral groups of lines from more than 60 SAQDs of the same sample. The energies of the various groups are presented in the figure as a function of the energy of the lowest spectral line A_1. A clear correlation between the various energies is observed. All the energies increase at the same rate so that the energy differences between the various groups remain more or less constant. As a result, the number of spectral groups of lines, which is associated with the number of discrete confined carriers' energy levels, decreases with the increase in the energy of the SAQD emission, since they are limited from above by the emission from the wetting layer. This clear correlation indicates that there is uniformity in the structural variables of the various SAQDs. Namely, the dimensions, compositions, and strain fields of the various dots are strongly correlated, and cannot be considered as statistically independent variables.

In Fig. 4(a), we present PL spectra of a single SAQD excited by picosecond short 1.750 eV laser pulses, at various excitation powers. The spectra, as measured in this case, represent the temporal average on the PL emission. Their evolution with increasing excitation power is similar to that observed in the cw excitation mode [Fig. 1(a)], except for one

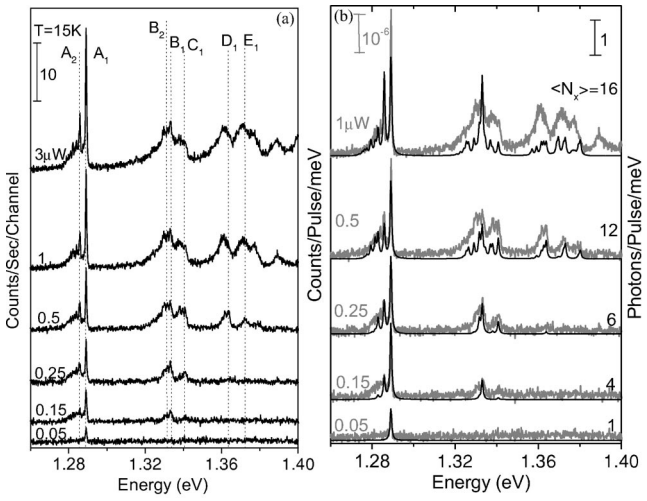

FIG. 4. Measured (a, and solid gray lines in b) and calculated (b, solid black lines, right axis) single SAQD PL spectra at various pulse excitation powers. The curves are vertically shifted for clarity.

significant difference. With the increase in excitation power, after reaching saturation, the intensity of the emission from the various spectral lines remains constant and it does not decrease with further increase in the excitation power. Our model simulations (see below) for this case are presented (by solid black lines, right axis) for comparison in Fig. 4(b), overlaid on the measured spectra (solid gray lines, left axis).

In Fig. 5(a) we present the PL intensity as a function of time after the excitation pulse at a given power, for various spectral lines from Fig. 4(a). In general, for each spectral line there are two distinct time domains. In the first one, the emission intensity rises with time after the excitation and in the second it decays. For a given excitation power, the various spectral lines have different temporal responses. As a rule, it is easily seen that the lower is the energy of a given spectral group of lines, the longer are their rise and decay times. Within a given group of lines, however, lower-energy lines rise and decay faster. Our model calculations (see below) are presented for comparison in Fig. 5(b). The rise time of a particular spectral line strongly depends on the excitation power. The higher the power is, the longer the rise time is, while the decay time is hardly affected. In Fig. 5(c) we display by symbols the measured rise time of the spectral lines A_1 and B_1 as a function of the excitation power. The lines in Fig. 5(d) represent our model calculations (see below).

IV. TIME EVOLUTION AND RECOMBINATION MODEL FOR MULTIEXCITONS

The PL emission spectrum of an optically excited semiconductor quantum dot results from optical transitions between multiexciton states.[11] The physical picture is as follows. The optical excitation generates a population of equal amounts of electrons and holes within the quantum dot. The many electron-hole pairs form a correlated multiexcitonic state. The photoexcited carriers reach thermal distribution on a very short time scale as compared with the time required for radiative recombination of an electron-hole pair. Thus, at low temperatures, the specific excited multiexciton state quickly relaxes to its ground multiexciton level. A radiative annihilation of one of the electron-hole pairs that composes the multiexciton may then occur by emission of a photon. This photon carries the energy difference between the energy of the initial (ground) multiexcitonic state and that of the final (possibly excited) new multiexcitonic state.

The energy carried by the photon is determined mainly by two factors. (a) The first is the single carrier energy level (shell) to which the annihilated electron-hole pair belongs. Thereby, the group of spectral lines which we denote by *A*, *B*, *C*, and *D* results from the annihilation of pairs in their first, second, third, and fourth single carrier energy levels, respectively.[10,11] Clearly, the larger is the number of pairs (i.e., the multiexciton order) within the SAQD, the more shells are occupied and consequently more groups of spectral lines constitute the PL spectrum. (b) Second, the number of ''spectator'' pairs, occupying the SAQD when the radiative annihilation occurs, determines the spectral position of the emitted photon within a given group of lines.[10,11] The larger the number of spectator pairs is, the lower is the spectral position of the emitted photon.[10,11] This is because the energy difference between successive multiexciton ground

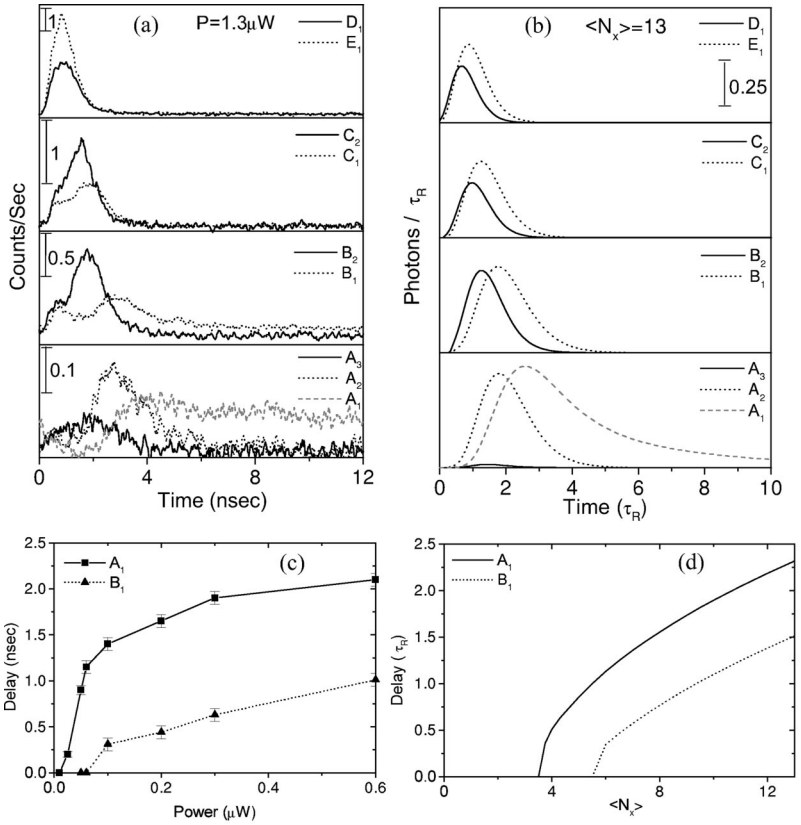

FIG. 5. Measured (a) and calculated (b) PL emission intensity as a function of time after the excitation pulse for various spectral lines from Fig. 4. Measured (c) and calculated (d) delay times of the spectral lines A_1 and B_1 as a function of excitation power (c) and average number of photogenerated QD excitons per pulse (d).

states is reduced by the sum of the electron-electron (e-e) and hole-hole (h-h) exchange terms, whenever the higher-order multiexciton is odd and therefore consists of an additional partially filled higher-energy shell. When the QD is occupied by an even number of pairs, only one spectral line results from the annihilation of a pair in a given shell (see Figs. 3 and 4 of Ref. 11). When there is an odd number of pairs, and thereby the highest energy shell of the multiexciton ground state is partially filled, up to three spectral lines may result from each such annihilation. The energy differences between these lines amount exactly to the sum of the e-e and h-h exchange terms between the partially filled shell and the shell of the annihilated pair.[11] Hence, the same spectral line may contain contributions from a few different multiexciton states. For example, the spectral line A_1 results from the annihilations of the single and the third multiexcitons, and the spectral lines A_2 and B_1 result from the annihilations of the third, fourth, and fifth multiexcitons. Similarly, the spectral lines B_2 and A_3 contain contributions from the annihilations of the fifth, sixth, and seventh multiexcitons. This relatively simple description of the optical transitions between confined multiexciton states is due to the fact that the differences between the multiexciton direct Coloumbic terms are much smaller than the exchange terms,[13] and therefore they are canceled out. The biexciton binding energy, which we find to be a fraction of the exchange energy between the first and second shells, is an exception. As a result, the annihilation of the biexciton ground state is spectrally unique. It solely results in the PL line A_{xx}.[11]

We note here that this simple description is model-dependent. Namely, the expected degeneracy of spectral lines due to different multiexciton annihilations is slightly removed when the spin-orbit interaction is taken into account.[22] This small degeneracy removal is certainly less than the typically measured PL spectral linewidth, and therefore it does not affect the analysis below.

Upon radiative recombination, the newly formed multiexcitonic state contains one less electron-hole pair and it quickly relaxes (nonradiatively) to its ground level. In the pulsed excitation mode, the process continues sequentially. A subsequent radiative pair annihilation occurs and the process continues, until the quantum dot remains empty from excitons, or another exciting pulse arrives. In the cw excitation mode, the number of excitons in the QD reaches a steady-state value, which depends on the rate at which e-h pairs are photogenerated.

At any given time only one, well defined, multiexciton may exist in the QD. We define by n_i $(0<n_i<1)$ the probability to find the ith multiexciton in the QD. Thus, for example, n_0 is the probability to find the QD empty, and n_2 is the probability to find a biexciton in the QD. We note the obvious sum rule for n_i:

$$\sum_{i=0}^{\infty} n_i = 1. \tag{1}$$

The temporal evolution of a multiexciton is described by the following rate equation:

$$\frac{dn_i}{dt} = G(t)n_{i-1} - \frac{n_i}{\tau_i} + \frac{n_{i+1}}{\tau_{i+1}} - g_{i+1}. \tag{2}$$

Here $G(t)$ is the total (time-dependent) QD exciton photogeneration rate, which corresponds to the power of the external excitation source at a given time and τ_i is the radiative lifetime of the ith multiexciton $(\tau_0=\infty)$. The first term sim-

ply expresses the idea that the photogeneration rate of the ith multiexciton linearly depends on the probability that the dot is occupied by the $(i-1)$th multiexciton. This means, of course, that the QD cannot be emptied by the excitation source (we neglect stimulated emission throughout this analysis). We note that in addition to the ''conventional'' first three terms in Eq. (2), there is also a fourth term which describes the decrease in the ith-multiexciton occupation probability due to the photogeneration of the $(i+1)$th multiexciton which causes the ith multiexciton to ''vanish.''

When the QD is photoexcited by a cw light source, G is time-independent, and the QD will reach a steady state in which $dn_i/dt=0$ for all i. By substituting this into Eq. (2), we get a set of linear equations which we solve analytically to yield $n_i(G)$ $(i>0)$,

$$n_i = n_0 G^i \prod_{j=1}^{i} \tau_j ,$$

$$n_0 = \frac{1}{1+\tau_1 G+\tau_1\tau_2 G^2+\cdots+G^N\prod_{j=1}^{N}\tau_j}, \tag{3}$$

where N is the highest-order multiexciton with nonvanishing occupation probability to be considered.

These coupled rate equations thus give rise to a peculiar feature of the multiexcitons: each multiexciton has its own distinguished dependence on the excitation density. We demonstrate these dependences in the calculated curves of Figs. 1(b) and 2(b). Using the calculated optical transitions from each multiexciton ground state (see below for details of the calculations), we calculate the PL emission spectrum of the SAQD under study. The calculated spectra (spectrally broadened by a Gaussian of 0.5 meV width) for various cw excitation densities are displayed in Fig. 1(b). In Fig. 2(b) we present the calculated emission strength of a few spectral lines as a function of the average steady-state number of photogenerated e-h pairs, $\langle N_x\rangle$. The figure demonstrates that the various spectral lines reach maximum at a comparable emission intensity, and that the spectrum shifts to the red as the excitation rate increases, in good agreement with the experimental observations.

We now turn to study the situation in which the QD is photoexcited by a temporally short laser pulse, with a repetition time that is much longer than the characteristic recombination time $(\simeq\tau_R)$. For simplicity, we assume immediate photogeneration of a well defined multiexciton following the pulse. This means that the photogeneration term (the first term) in Eq. (1) is now given by $\delta(\mathrm{t})\,\delta_{N_p,i}$, where N_p is the number of photoexcited excitons in the QD per each laser pulse. The temporal evolution of a given multiexcitonic occupation probability for this case is obtained in a straightforward manner using the analytic solution of Eq. (1), which yields

$$n_i(t)=\begin{cases} \displaystyle\sum_{k=1}^{N_p}\frac{\tau_k^{(N_p-1)}}{\displaystyle\prod_{j=1,j\neq k}^{N_p}(\tau_k-\tau_j)}(1-e^{-t/\tau_k}), & i=0,\\ \displaystyle\sum_{k=i}^{N_p}\frac{\tau_k^{(N_p-i-1)}\tau_i}{\displaystyle\prod_{j=1,j\neq k}^{N_p}(\tau_k-\tau_j)}e^{-t/\tau_k}, & 0<i\leqslant N_p,\\ 0, & i>N_p. \end{cases} \tag{4}$$

For the purpose of comparison with the temporally integrated PL measurements [Fig. 4(a)], we temporally integrate Eq. (4) to yield the probability R_i for the ith multiexciton to recombine radiatively after the pulsed excitation,

$$R_i=\frac{1}{\tau_i}\int_0^\infty n_i(t)dt=\sum_{k=i}^{N_p}\frac{\tau_k^{(N_p-1)}}{\displaystyle\prod_{j=1,j\neq k}^{N_p}(\tau_k-\tau_j)}=\begin{cases}1, & 0<i\leqslant N_p\\ 0, & i>N_p.\end{cases} \tag{5}$$

As expected, R_i is unity for all $i\leqslant N_p$. Thus, in order to obtain the measured pulsed spectrum, we simply sum over all the allowed optical transitions of these multiexcitons. These sums are given for the first few multiexcitons in the last row of Table II. The calculated spectra for various excitation densities are presented in Fig. 4(b). We note here that in the calculations of Fig. 4(b) we accounted for the statistical nature of the photoexcitation process. Thus, the probability to photogenerate N_p excitons in the QD is given by

$$P(N_p)=\frac{\exp\left(-\dfrac{2(N_p-\langle N_x\rangle)^2}{\langle N_x\rangle}\right)}{\displaystyle\sum_{j\geqslant 0}\exp\left(-\frac{2(j-\langle N_x\rangle)^2}{\langle N_x\rangle}\right)}, \quad N_p=0,1,2,\ldots, \tag{6}$$

where here $\langle N_x\rangle$ is the average number of photogenerated QD excitons per laser pulse.

Our model emphasizes an important feature of pulsed excitations, namely, the average number of excitons within the SAQD, during the lifetime of the photogenerated carriers, is considerably larger than that in the cw case. Furthermore, the temporally integrated probability for a given multiexciton to actually recombine is exactly 1. For that reason, already at very low excitation power, many characteristic spectral lines are observed and, unlike the cw case, their intensity does not decrease with increasing excitation power.

V. DISCUSSION

The complex task of calculating the emission spectrum which results from the radiative annihilation of a multicarrier state can be quite well approximated provided that the energy levels of single carriers within the dots are known and that, in addition, the exchange integrals between these levels are known as well.[11] In order to calculate these values, an exact knowledge of the quantum-dot dimensions, geometrical shape, composition, and strain field has to be known.[23–25] At this stage, it is unrealistic to expect such a detailed knowl-

TABLE I. Calculated exchange energies between single confined carrier states within the SAQD.

j	Δ_{2j} (eV)	Δ_{3j} (eV)	Δ_{4j} (eV)	Δ_{5j} (eV)	Δ_{6j} (eV)	Δ_{7j} (eV)	Δ_{8j} (eV)
1	1.7	1.6	0.76	1.1	1.0	0.58	0.55
2		0.76	1.4	1.4	0.55	0.63	0.89
3			1.5	0.58	1.3	0.98	0.62
4				0.63	0.62	1.2	1.1
5					0.46	1.3	0.47
6						0.48	1.4
7							0.52

edge for each SAQD. Fortunately, these energies can be, to a large extent, deduced directly from the measured QD emission spectrum. For example, it is quite obvious that the single line observed at low excitation density (line A_1) is due to the recombination of a single exciton within the optically excited SAQD. Similarly, it follows that the first line in the higher-energy group of spectral lines (line B_1) is due to the recombination of an electron-hole pair in their respective second energy levels. Lines C_1 and D_1 similarly mark higher-energy optical transitions due to the recombination of electron-hole pairs at their respective third and fourth single carrier energy levels. As discussed above and demonstrated in Ref. 10, the combined electron-electron and hole-hole exchange energy between their first and second single carrier levels is given precisely by the energy difference between line A_1 and line A_2. Similarly, the energy difference between the spectral lines B_1 and B_2 is an exact measure for the combined exchange energy between the first and third single carrier energy states. We emphasize here again that the spectral line A_2 acquires contributions from the recombinations of the third, fourth, and fifth multiexcitons.[10,11] Line A_2 does *not* originate from the recombination of the biexciton. The so-called ''biexciton'' spectral line is the line that we denote by A_{xx}. It is split downward in energy from the single exciton line A_1 by the biexcitonic binding energy. Our model calculations show that this energy amounts only to about 20% of the A_2-A_1 exchange splitting, in agreement with others.[13,22,26,27] Moreover, since the biexciton PL line acquires contribution from the recombination of the biexciton only, its excitation density dependence is different from that of the other spectral lines in group *A*, as correctly given by our model.

In Table I we present the exchange energies calculated for a simple geometrical shape for the SAQD.[10,11] We found out that these integrals are not particularly sensitive to the geometrical shape of the QD. Therefore, the knowledge of one or two exchange terms can be used for deducing the rest of these terms.

The e-e and h-h exchange interactions are responsible for the line splitting described in Figs. 1(a) and 4(a). In addition, they give rise to a spectral redshift of optical transitions from successively higher-order multiexcitons, as we demonstrated previously.[10] This redshift is caused by the number of exchange interactions, which increases with the number of carriers. Therefore, the sum of exchange interaction energies lowers the energy of the $N+1$ multiexciton levels more than it lowers the energy of the N multiexciton levels, thus causing a successive redshift in the transition energies.

In order to understand the spectral evolution of the SAQD PL with excitation density and with time after pulse excitation, knowledge of the various recombination rates of a particular multiexcitonic state is required. A realistic estimate of these rates is obtained using the following simplifications.

(a) We consider optical transitions in which a photon is emitted as a result of the annihilation of one electron-hole pair.

(b) For these cases we use the dipole approximation for calculating the optical transition rate between initial and final multiexcitonic states.

(c) We further assume that the dipole matrix element for optically allowed transitions between single carrier states is equal to that of the single exciton τ_R.[10,11]

(d) Since the change in the total spin and its projection along the growth axis is ''taken up'' by the electron and hole Bloch functions,[10,13] optical transitions can occur only between multiexcitonic states of the same total spin and the same spin projection along the growth axis. The optical recombination rates can thus be easily estimated by summing the angular momentum and symmetry-conserving transitions between the initial to the final states and by averaging over all the initial states.

(e) We assume that the QD is in thermal equilibrium when photons are emitted due to exciton annihilation. Therefore, only optical transitions from the ground energy level of each $(N+1)$th multiexciton to all possible levels of the Nth multiexciton are considered. Therefore, the reciprocal of the sum of all the recombination rates of a multiexciton ground state constitutes its lifetime.

In Table II, we list the estimated radiative rates of the first QD multiexcitons. These rates are given in units of the radiative rate of the QD single exciton (τ_R^{-1}). The table also lists the radiative recombination rates of each multiexciton to the various spectral lines. We note that a decaying multiexciton contributes to a few spectral lines, and that each spectral line may acquire contributions from the radiative recombination of a few multiexcitons. The last row of Table II contains the sum over all the radiative contributions of the various sequentially decaying multiexcitons to a given spectral line. In the calculation of these sums, the conditions of Eq. (5) apply. Therefore, these rates represent the relative intensities of the saturated PL spectral lines for pulsed excitation.

The calculated temporal dependence of the emission intensity of a few spectral lines and a given $\langle N_x \rangle$ is displayed in Fig. 4(b). The calculations yield very good agreement with the measured spectra [Fig. 4(a)]. In particular, it is worth noting that the multiexciton model explains the rise time of the various spectral lines and its dependence on the excitation density [Fig. 4(c)]. Consider, as an example, the spectral line A_1. According to the model,[11] as can be seen in Table II, this line originates from the recombination of either a single exciton or the third multiexciton (triexciton). For a larger multiexciton, the annihilation of the corresponding electron-hole pair results in a redshifted line (such as A_2 and A_3). Therefore, if the excitation pulse photogenerates more than three excitons in the QD, the appearance of the A_1 line will be delayed in time. It will only appear after enough radiative annihilations of electron-hole pairs have occurred such that

TABLE II. Estimated total and partial QD multiexciton radiative decay rates to the various spectral lines (in units of τ_R^{-1}). The sums in the last row, therefore, represent the relative intensities of the various spectral lines at saturation under pulse excitation (see text).

i	A_1	A_{xx}	A_2	A_3	A_4	A_5	B_1	B_2	B_3	C_1	C_2	C_3	D_1	τ_i^{-1}
1	$\frac{1}{4}$													$\frac{1}{4}$
2		$\frac{8}{4}$												2
3	$\frac{18}{4}$		$\frac{12}{4}$	$\frac{2}{4}$			$\frac{4}{4}$							9
4			$\frac{8}{4}$				$\frac{8}{4}$							4
5			$\frac{18}{4}$	$\frac{12}{4}$	$\frac{2}{4}$		$\frac{18}{4}$	$\frac{12}{4}$	$\frac{2}{4}$	$\frac{4}{4}$				17
6				$\frac{8}{4}$				$\frac{8}{4}$		$\frac{8}{4}$				6
7				$\frac{18}{4}$	$\frac{12}{4}$	$\frac{2}{4}$		$\frac{18}{4}$	$\frac{12}{4}$	$\frac{18}{4}$	$\frac{12}{4}$	$\frac{2}{4}$	$\frac{4}{4}$	25
8					$\frac{8}{4}$				$\frac{8}{4}$		$\frac{8}{4}$		$\frac{8}{4}$	8
rel. int.	1.50	1.00	1.10	0.75	0.52	0.41	0.88	0.69	0.52	0.57	0.49	0.41	0.41	

all but three excitons have recombined. The larger the intensity of the exciting pulse is, the more excitons are initially photogenerated. Therefore, the rise times increase strongly with the pulse intensity. In addition, since higher-energy groups of spectral lines are associated with larger multiexcitons, their rise times are shorter.

We now turn to estimate the radiative lifetime of the SAQD single exciton ($\tau_1 = 4\tau_R$). This task cannot be simply accomplished by measuring the decay time of the spectral line A_1, since low light level emission rates are very sensitive to nonradiative recombination channels.[11] The rise times and their excitation intensity dependence, however, are much less sensitive to the presence of saturable nonradiative channels. Therefore, from the comparison between the measured and calculated rise times as a function of excitation density [Fig. 3(c)], τ_1 is straightforwardly estimated to be 4 nsec. This surprisingly long lifetime is also verified by yet another independent estimation. From the magnitude of the temporally integrated PL emission in which the distinct spectral lines saturate under pulse excitation, the efficiency of our collection optics can be directly found [see Eq. (5) and Fig. 2(b)]. The determined efficiency is now used to obtain τ_R from the maximal intensity of the spectral line A_1 in cw excitation (see Fig. 2). Both methods agree to within a factor of 2 and they do not require knowledge of the excitation efficiency (i.e., the relation between $\langle N_x \rangle$ and the excitation density).

VI. SUMMARY

We applied low-temperature diffraction-limited confocal optical microscopy to spatially resolve and spectroscopically study photoluminescence emission from single self-assembled InAs/GaAs quantum dots.

The measured spectra and their dependences on time and excitation intensity are measured and analyzed using a theoretical multiexcitonic model. The input parameters for the model are the single carrier level energies and the exchange energies between these levels. We show that our model with this minimal set of parameters, which we directly deduced from the measured spectra, quantitatively describes the evolution of the photoluminescence spectrum of an optically excited single semiconductor quantum dot as a function of excitation density and time after its pulsed excitation.

ACKNOWLEDGMENTS

The research was supported by the US-Israel Binational Science Foundation (453/97) and by the Israel Science Foundation founded by the Israel Academy of Sciences and Humanities.

[1] U. Bockelmann, W. Heller, A. Filoramo, and P. Roussignol, Phys. Rev. B **55**, 4456 (1997).
[2] K. Brunner, G. Abstreiter, G. Bohm, G. Trankle, and G. Weimann, Phys. Rev. Lett. **73**, 1138 (1994).
[3] D. Gammon, E.S. Snow, B.V. Shanabrook, D.S. Katzer, and D. Park, Phys. Rev. Lett. **76**, 3005 (1996).
[4] W. Wegscheider, G. Schedelbeck, G. Abstreiter, M. Rother, and M. Bichler, Phys. Rev. Lett. **79**, 1917 (1997).
[5] Q. Wu and R.D. Grober, Phys. Rev. Lett. **83**, 2652 (1999).
[6] M. Bayer, T. Gutbrod, A. Forchel, V.D. Kulakovskii, A. Gorbunov, M. Michel, R. Steffen, and K.H. Wang, Phys. Rev. B **58**, 4740 (1998).
[7] A. Zrenner, M. Markmann, A. Paassen, A.L. Efros, M. Bichler, W. Wegscheider, G. Böhm, and G. Abstreiter, Physica B **256-258**, 300 (1998).
[8] L. Landin, M.-E. Pistol, C. Pryor, M. Persson, L. Samuelson, and M. Miller, Phys. Rev. B **60**, 16 640 (1999).
[9] Y. Toda, O. Moriwaki, M. Nishioka, and Y. Arakawa, Phys. Rev. Lett. **82**, 4114 (1999).
[10] E. Dekel, D. Gershoni, E. Ehrenfreund, D. Spektor, J.M. Garcia, and P.M. Petroff, Phys. Rev. Lett. **80**, 4991 (1998).
[11] E. Dekel, D. Gershoni, E. Ehrenfreund, D. Spektor, J.M. Garcia, and P.M. Petroff, Phys. Rev. B **61**, 11 009 (2000).
[12] A. Wojs and P. Hawrylak, Phys. Rev. B **55**, 13 066 (1997).
[13] A. Barenco and M.A. Dupertuis, Phys. Rev. B **52**, 2766 (1995).
[14] I. Shtrichman, D. Gershoni, and R. Kalish, Phys. Rev. B **56**, 1509 (1997).
[15] G. Bacher, R. Weigand, V.D. Kulakovskii, N.A. Gippius, A. Forchel, K. Leonardi, and D. Hommel, Phys. Rev. Lett. **83**, 4417 (1999).

[16] V. Zwiller, M.E. Pistol, D. Hessman, R. Cederstrom, W. Seifer, and L. Samuelson, Phys. Rev. B **59**, 5021 (1999).
[17] L.M. Robinson, H. Rho, J.C. Kim, H.E. Jackson, L.M. Smith, S. Lee, M. Dobrowolska, and J.K. Furdyna, Phys. Rev. Lett. **83**, 2797 (1999).
[18] V.I. Klimov, A.A. Mikhailovsky, D.W. McBranch, C.A. Leatherdale, and M.G. Bawendi, Science **287**, 101 (2000).
[19] I.N. Stranski and L. Krastanov, Akad. Wiss. Lit. Mainz Abh. Math. Naturwiss. Kl. **146**, 767 (1939).
[20] J.M. Garcia, T. Mankad, P.O. Holtz, P.J. Wellman, and P.M. Petroff, Appl. Phys. Lett. **72**, 3172 (1998).
[21] The relation between this notation and the one we used in Ref. 11 is the following: A_2, A_1, B_2, and B_1 in this work correspond to line number 1, 2, 4, and 5, respectively, in Ref. 11.
[22] A. Williamson, A. Franceschetti, and A. Zunger, cond-mat/0003188 (unpublished).
[23] L.W. Wang, J. Kim, and A. Zunger, Phys. Rev. B **59**, 5678 (1999).
[24] O. Stier, M. Grundmann and D. Bimberg, Phys. Rev. B **59**, 5688 (1999).
[25] C. Pryor, Phys. Rev. B **60**, 2869 (1999).
[26] T. Takagahara, Phys. Rev. B **39**, 10 206 (1989).
[27] Y.Z. Hu, S.W. Koch, M. Lindberg, N. Peyhambarian, E.L. Pollock, and F.F. Abraham, Phys. Rev. Lett. **64**, 1805 (1990).